32ND INTERNATIONAL COSMIC RAY CONFERENCE, BEIJING 2011

Energy Dependence of the Large Scale Galactic Cosmic Rays Anisotropy Measured With IceCube

THE ICECUBE COLLABORATION[1]
[1]*See special section in these proceedings*

Abstract: We report on a study of the energy dependence in the arrival direction distribution of cosmic rays at median energies of 20 and 400 TeV. The data used in this analysis contain 33×10^9 downward going muon events collected by the IceCube neutrino observatory between May 2009 and May 2010 when it comprised of 59 strings. The high rate of cosmic ray induced muons observed by IceCube allows us to perform the first study of the galactic cosmic ray arrival distribution around 400 TeV in the Southern sky. The sidereal anisotropy observed at 400 TeV shows substantial differences with respect to that at lower energy. Studies of the energy dependence of the anisotropy could further enhance the understanding of the structure of the local interstellar magnetic field and possible nearby cosmic ray sources.

Corresponding Authors: Rasha Abbasi[2](*rasha.abbasi@icecube.wisc.edu*), Paolo Desiati[2](*desiati@icecube.wisc.edu*)
[2]*Dept. of Physics, University of Wisconsin-Madison, Madison, WI 53703, USA*

Keywords: IceCube, Cosmic Rays, Anisotropy, Muons, Neutrinos.

1 Introduction

During the last decades, Galactic cosmic rays have been found to have a small but measurable energy dependent sidereal anisotropy in their arrival direction distribution with a relative amplitude of order of 10^{-4} to 10^{-3}. The first comprehensive observation of the cosmic ray sidereal anisotropy was provided by a network of muon detectors sensitive to cosmic rays between 10 and several hundred GeV [1]. More recent underground and surface array experiments in the Northern hemisphere have shown that a sidereal anisotropy is present in the TeV energy range (i.e. Tibet Air Shower Arrays (Tibet ASγ) [2], Milagro [3]). The IceCube neutrino observatory reported for the first time the observation of the cosmic rays sidereal anisotropy in the Southern sky at energies in excess of about 10 TeV [4]. The cosmic ray anisotropy reported by IceCube showed that the large scale features were a continuation of those observed in the Northern hemisphere in the same energy range.

At high energies, the Tibet ASγ collaboration reported the non-observation of a sidereal anisotropy in the cosmic ray arrival direction distribution at $\sim$ 300 TeV [2]. Another measurement at $\sim$370 TeV was recently published by the EAS-TOP collaboration reporting a larger sidereal anisotropy in amplitude with a shift in phase from that observed at lower energies [5]. At this point the two observations do not provide a coherent picture of the sidereal anisotropy at high energy in the Northern hemisphere.

In this contribution we present the analysis and the results of the study of large scale cosmic ray anisotropy at median energies of 20 and 400 TeV by IceCube for the Southern celestial sky. Observations of the energy dependence of the anisotropy could provide us with further information for the development of theoretical models to better understand the origin and propagation of cosmic rays.

2 Data Analysis

The main goal of the IceCube neutrino observatory is to detect astrophysical neutrinos. Neutrinos passing through the Earth and interacting in the vicinity of IceCube produce muons or other secondaries that emit Cherenkov radiation in the clear ice surrounding the detector. It is these light signals that the IceCube optical modules record. On the other hand, muons produced by cosmic ray air-showers in the atmosphere above IceCube are also detected. These are observed as down-going tracks.

The data used in this analysis are the downward going muons collected by the IceCube detector comprising 59 strings. The data were collected from May 2009 to May 2010 [6]. The events used in this analysis are those reconstructed by an online likelihood based reconstruction algorithm at an average rate of $\sim$1250 Hz with a median

angular resolution of $\sim 3^\circ$. A range of selection criteria is applied to that data to ensure good quality and stable runs. The final data set consists of 33×10^9 events corresponding to a detector livetime of 324.8 days.

Due to the detector's unique location, the IceCube Observatory has full coverage of the Southern sky up to declination angles of -25° degrees at any time of the year. The seasonal and atmospheric variation of the muon intensity were found to occur uniformly across the entire field of view, and therefore it did not affect the arrival distribution of the reconstructed events [4]. The crucial effect that needed to be accounted for was due to the geometrical shape of IceCube: events that were parallel to a larger number of strings were more efficiently reconstructed. The non-uniform time coverage due to detector downtime and run selection precluded the complete averaging of the detector geometrical asymmetry and generated artificial variations of the arrival direction of cosmic rays in equatorial coordinates. The local azimuthal asymmetry was corrected by reweighting the arrival directions of the data [4].

3 Energy Estimation

The energy dependence of the large scale anisotropy may hint at the nature of the source (or sources) of the cosmic rays, as well as their propagation through galactic magnetic fields. Similar measurements have been carried out over a wide range of energies by underground muon experiments and air shower arrays [1, 7, 8, 9, 10] but there are relatively few observations in the multi-TeV region.

Since IceCube detects cosmic ray properties indirectly through the observation of muons produced in the extensive air showers, the cosmic ray particles energy is inferred from the estimation of the muon energy. In this analysis, we use the number of optical modules Nch participating together with the zenith angle θ of the event to estimate the energy of the events. Using Monte Carlo simulations, we have identified cuts of constant energy in (Nch, θ) for the two event samples. The primary cosmic ray energy estimation had a resolution of about 0.5 in $\log_{10}$ scale and, this is due to the fact that it is dominated by the large fluctuations of the number and energy of muons produced in the extensive air showers. The low energy sample contained events with a median energy of 20 TeV, where 68% of the events were between $4-63$ TeV; and the high energy sample contained events with a median energy of 400 TeV, were 68% of the events were between $100-1258$ TeV.

4 Results

To investigate the arrival direction distribution of the cosmic rays, we study the relative intensity of the cosmic ray flux. The arrival direction distribution is dominated by the zenith angle dependence of the flux. Therefore, we normalize the flux within declination belts of width $\sim 3^\circ$, which corresponds to the angular resolution of the data.

To quantify the scale of the anisotropy, we fitted the right ascension projection distribution for declinations angles -25°to -75° degrees of the data to a first and second-order harmonic function of the form

$$\sum_{j=1}^{2} A_j \cos[j(\alpha-\phi_j)] + B \qquad (1)$$

where (A_i, ϕ_i) are the amplitude and phase of the anisotropy, α is the right ascension, and B is a constant. Figures 1 and 2 show the relative intensity cosmic ray maps together with the profile of the data in right ascension for events in both the 20 TeV and the 400 TeV energy sample. The error bars in the right ascension projection are derived by propagating the statistical errors from each declination belt, and the gray band indicates the estimated maximal systematic uncertainties (described in section 4.1.1). The solid line indicates the fit of eq. (1) to the data. The first and second harmonic amplitude and phase of the sidereal anisotropy for the low energy sample together with their statistical and systematic uncertainties are $A_1 = (7.9\pm0.1_{stat.}\pm0.4_{syst.})\times10^{-4}$ and $\phi_1 = 50.5^\circ\pm1.0^\circ_{stat}\pm 1.1^\circ_{syst.}$, $A_2 = (2.9\pm0.1_{stat.}\pm0.4_{syst.})\times10^{-4}$ and $\phi_2 = 299.5^\circ \pm 1.3^\circ_{stat} \pm 1.5^\circ_{syst.}$. While those for the high energy sample are $A_1 = (3.7\pm0.7_{stat.}\pm0.7_{syst.})\times10^{-4}$ and $\phi_1 = 239.2^\circ\pm10.6^\circ_{stat}\pm10.8^\circ_{syst.}$, $A_2 = (2.7\pm0.7_{stat.}\pm 0.6_{syst.})\times10^{-4}$ and $\phi_2 = 152.7^\circ \pm 7.0^\circ_{stat} \pm 4.2^\circ_{syst.}$.

4.1 Reliability Checks

4.1.1 Data Stability

In order to assess and quantify the systematic uncertainties in the sidereal anisotropy of cosmic ray arrival direction distribution a number of checks were applied by dividing the low and high energy data samples in exclusive halves based on different criteria. A full analysis was then applied for each dataset and the relative intensity distribution in right ascension was determined for each of them. The stability checks applied are:

- Seasonal variations dependence: where the data was divided in two seasons (winter and summer).
- Rate variations dependence: where the data was divided for each day by the sub-run (a sub-run corresponded to approximately 2 minutes of observations) rate fluctuating being greater than or less than the median rate of the day.
- Choices of events sample dependence: where the data was divided by the sub-run number using multiple categories.
- Non-uniform time coverage dependence due to detector down time and quality run selection: where the analysis was performed on the sub-sample of days with maximal data collection time.

The sidereal distribution of relative intensity in the arrival direction of the cosmic rays for the low and high energy samples are used to evaluate the spread in the experimental observation from the full-year event samples. The gray bands in the right ascension projection in Figures 1 and 2 describe the maximal spread obtained from the result of all the stability checks described in this section.

4.1.2 Solar Diurnal Anisotropy

To test for the stability of the observatory and its time coverage, an effective way to have an absolute calibration of the experimental sensitivity for the detection of the sidereal directional asymmetries is to measure the solar anisotropy from the Earth's revolution around the Sun. This observation has solid theoretical grounds and it was first reported in 1986 [11] and then later observed by multiple experiments in the multi-TeV energy range (i.e. [2], [3]). The observed solar anisotropy is consistent with a dipole that describes an apparent excess of cosmic rays in the direction of Earth's motion around the Sun and a deficit in the opposite direction.

Figure 3 shows the projections of the cosmic ray arrival direction in solar reference frame, for both energy samples (20 and 400 TeV). The error bars are the statistical errors, and the shaded bands indicate the expectation of the dipole. A fit to the projection of relative intensity distribution is shown by the black line and was done using the first harmonic term of eq. (1). The figures show that the experimental observation of the solar dipole is consistent with the expectations in both amplitude and phase. This observation of the solar diurnal anisotropy supports the reliability of the sidereal anisotropy determination.

4.1.3 Anti-sidereal Anisotropy

An annual modulation in the amplitude of the solar anisotropy is expected to result in a spurious effect in the sidereal anisotropy. This would produce a bias in the observed sidereal anisotropy. To estimate this bias the so-called anti-sidereal time, i.e. a non-physical time frame obtained by reversing the sign of the transformation from solar time to sidereal time [12].

Figure 4 shows the projections of the cosmic ray arrival direction in anti-sidereal reference frame, for both energy samples (20 and 400 TeV). The error bars are the statistical errors. The distributions were then fitted to the dipole term of eq. (1). The uncertainty in the first harmonic amplitude and phase implied by the study in the anti-sidereal time frame is within the statistical and systematic errors determined from the data stability tests. The absence of the signal in the anti-sidereal time insures the reliability of the anisotropy observed in sidereal time.

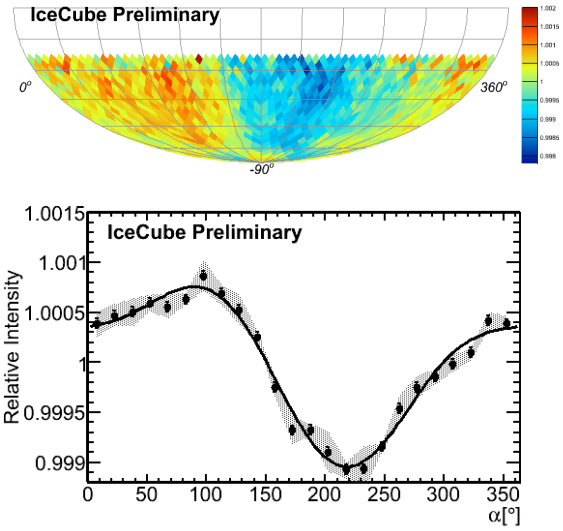

Figure 1: The top figure is the IceCube relative intensity cosmic ray map for the low energy sample (Median energy of the primary cosmic ray particle of 20 TeV). The bottom figure is the one dimensional projection in right ascension α of the two-dimensional cosmic ray map. The black line corresponds to the first and second harmonic fit to the data. The gray band indicates the estimated maximal systematic uncertainties.

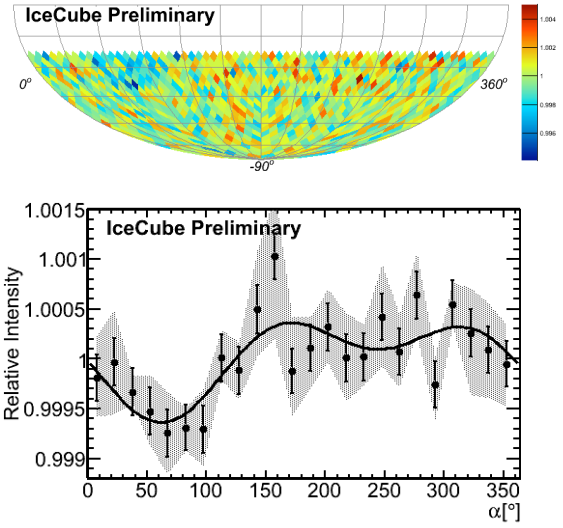

Figure 2: The top figure is the IceCube relative intensity cosmic ray map for the high energy sample (Median energy of the primary cosmic ray particle of 400 TeV). The bottom figures is the one dimensional projection in right ascension α of the two-dimensional cosmic ray map. The black line corresponds to the first and second harmonic fit to the data. The gray band indicates the estimated maximal systematic uncertainties.

5 Conclusion

In this contribution we presented the results on the large scale cosmic ray sidereal anisotropy at cosmic ray median

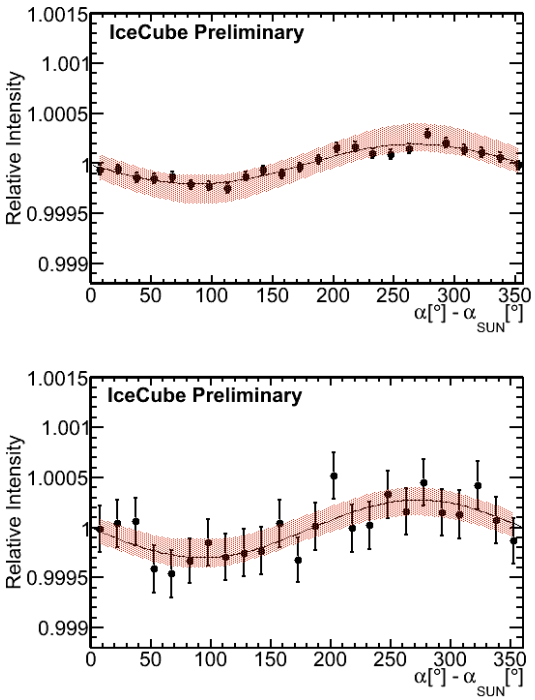

Figure 3: The solar projections for cosmic rays with median energy of 20 TeV (The top figure) and 400 TeV (The bottom figure). The error bars are the statistical errors, and the shaded band indicated the solar diurnal dipole expected from the motion of the Earth around the Sun.

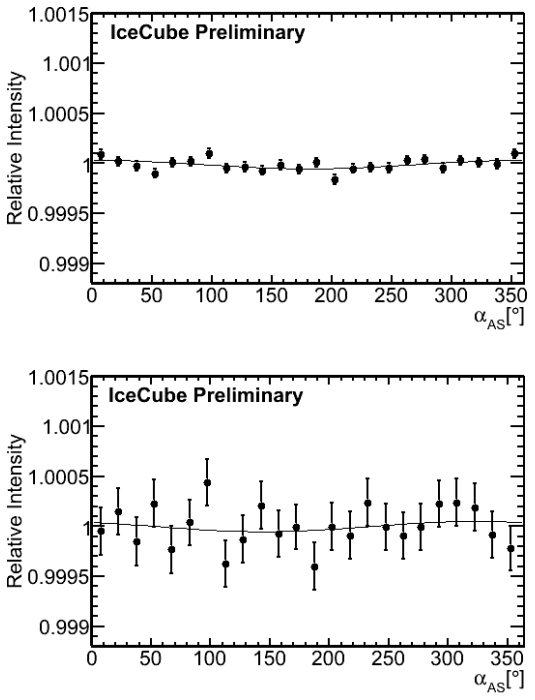

Figure 4: The anti-sidereal projections for cosmic rays with median energy of 20 TeV (The top figure) and 400 TeV (The bottom figure). The error bars are the statistical errors. The black line corresponds to the first harmonic fit to the data.

energies of 20 TeV and 400 TeV. The source of the sidereal anisotropy is still unknown. It is believed that a possible contribution to this observed anisotropy might be from the Compton-Getting effect, due to the orbital motion of the solar system around the galactic disk. However, the sidereal anisotropy from both energy samples do not appear to be consistent with that expected from the suggested Compton-Getting model neither in amplitude nor in phase.

The sidereal anisotropy observed at 20 TeV with IceCube-59 is consistent with the previously reported observation with IceCube [4], thus providing a confirmation of an apparent continuation of the arrival distribution pattern observed in the Northern hemisphere. On the other hand the sidereal anisotropy observed at 400 TeV shows substantial differences with respect to that at lower energy. The anisotropy at high energy shows a relative deficit region in right ascension where the broad excess dominated at primary median energy of 20 TeV. Also the wide relative deficit region at low energy seemed to have disappeared at primary median energy of 400 TeV. Whatever generated the sidereal anisotropy at 20 TeV seems to have no effect at 400 TeV.

This is the first observation of the sidereal anisotropy at 400 TeV in the Southern hemisphere. We are continuously analyzing events from IceCube with updated configurations. IceCube construction is now completed with 86 strings deployed with a volume of km^3 in January of 2011. With the higher statistical power expected from the observed cosmic ray muons we will be able to improve our understanding of the energy dependence of the anisotropy with more significance and close to the knee region. The energy dependence of the cosmic ray anisotropy is vital to our understanding of the source and propagation of cosmic rays.

References

[1] Nagashima et al., J. Geophys. Res., 1998, **103**: 17429.
[2] Amenomori et al., Science, 2006, **314**:439.
[3] Abdo et al., Astrophys. J., 2009, **698**:2121.
[4] Abbasi et al., Astrophys. J., 2010, **718**:L194.
[5] Aglietta et al., Astrophys. J., 2009, **692**:130.
[6] Abbasi et al., arXiv:1105.2326.
[7] Bercovitch, M., et al., International Cosmic Ray Conference,1981, **67**: 246.
[8] Cutler, D. J., et al., Astrophys. J., 1991, **376**: 322.
[9] Andreyev, Y. M., et al., International Cosmic Ray Conference, 1987, **2**: 22.
[10] Munakata, K., et al., International Cosmic Ray Conference,1999, **7**: 293.
[11] Cutler, D. J., & Groom, D. E., Nature, 1986,**322**: 434.
[12] Farley, F. J. M., & Storey, J. R., Proc. Phys. Soc., 1954,**67**: 996.
[13] Redfield, S., & Linsky, J. L., Astrophys. J., 2000,**534**: 825.